

Article

Linear versus nonlinear acoustic probing of plasticity in metals: A quantitative assessment

Carolina Espinoza ^{1,*}, Daniel Feliú ¹, Claudio Aguilar ², Rodrigo Espinoza-González ³, Fernando Lund ¹, Vicente Salinas ^{1,4} and Nicolás Mujica ¹

¹ Departamento de Física, Facultad de Ciencias Físicas y Matemáticas, Universidad de Chile, Avenida Blanco Encalada 2008, Santiago, Chile

² Departamento de Ingeniería Metalúrgica y Materiales, Universidad Técnica Federico Santa María, Av. España 1680, Valparaíso, Chile

³ Departamento de Ingeniería Química, Biotecnología y Materiales, Facultad de Ciencias Físicas y Matemáticas, Universidad de Chile, Avenida Beauchef 851, Santiago, Chile

⁴ Núcleo de Matemáticas, Física y Estadística, Facultad de Estudios Interdisciplinarios, Universidad Mayor, Manuel Montt 318, Providencia, Chile

* Correspondence: carolinaespinoza@ug.uchile.cl; Tel.: +56 9 6965 4363

Abstract: The relative dislocation density of aluminum and copper samples is quantitatively measured using linear Resonant Ultrasound Spectroscopy (RUS). For each metallic group, four samples were prepared with different thermomechanical treatments in order to induce changes in their dislocation densities. The RUS results are compared with Nonlinear Resonant Ultrasound Spectroscopy (NRUS) as well as Second Harmonic Generation (SHG) measurements. NRUS has a higher sensitivity by a factor of two to six and SHG by 14% to 62%. The latter technique is, however, faster and simpler. As main a result we obtain a quantitative relation between the changes in the nonlinear parameters and the dislocation density variations, which in a first approximation is a linear relation between these differences. We also present a simple theoretical expression that explains the better sensitivity to dislocation content of the nonlinear parameters with respect to the linear ones. X-Ray diffraction measurements, although intrusive and less accurate, support the acoustics results.

Keywords: alloys; nondestructive testing; dislocation density; plasticity; ultrasound; nonlinear acoustics

1. Introduction

Dislocation density is a key variable to describe and, possibly, to control, the plastic behavior of metallic materials. In situ measurement of plastic behavior and thus, directly or indirectly, of dislocation density, has been a particularly active area of research in recent years, especially at the micro and nano scale, using transmission electron microscopy (TEM), scanning electron microscopy (SEM) and atomic force microscopy (AFM). For example, in-situ TEM has been used to perform tensile tests of submicrometer aluminum single crystals [1], to test single crystal aluminum to study the evolution of dislocation patterns [2], to determine the relation between the evolution of the dislocation structures and the flow stress during compression of steel nanoblades [3] and to study dislocation emission in stainless steel [4]. However, these are destructive techniques and, in general, small, specially prepared samples are required. In most engineering applications these conditions can not be satisfied. Therefore, in situ and non-destructive tests are desirable.

Acoustics has long been a tool for the non-destructive evaluation of materials [5–8]. It is routinely used for crack detection [9–12]. However, concerning the plastic behavior of metals and alloys, it is only recently that progress in theoretical modeling and instrumentation development have enabled acoustic measurements to emerge as a quantitative tool to measure dislocation density. On the theory side, Maurel et al., [13,14], building on the classic work of Granato and Lücker [15] derived the following

formula, valid for isotropic materials, that relate the change in dislocation density between two samples with the change in the speed of shear waves and with the change in the speed of sound waves:

$$\frac{\Delta v_T}{v_T} = -\frac{8}{5\pi^4} \Delta(nL^3) = -\frac{8}{5\pi^4} \Delta(\Lambda L^2), \quad (1)$$

where $\Delta v_T/v_T$ is the relative change of shear wave velocity between two samples of a material that differ in dislocation density $\Lambda = nL$, and n is the number of dislocation segments of (average) length L per unit volume. This is an extremely simple result that was experimentally verified using Resonant Ultrasound Spectroscopy (RUS) [16] by Mujica et al. [17]. In addition, Salinas et al. [18] measured nL^3 in-situ and continuously as a function of applied stress for aluminum under standard testing conditions. These measurements provided an experimental verification of Taylor's rule with unprecedented accuracy [18]. They provide a solid basis to use velocity measurements as a nonintrusive quantitative measure, as opposed to qualitative estimate, changes in dislocation density. From a purely conceptual point of view, it is interesting to notice that the relevant dimensionless parameter that measure dislocation density is nL^3 .

Armed with this new tool, we can use it to assess the accuracy of other proposed techniques to determine dislocation density. For example, nonlinear methods have been proposed because of their potentially superior sensitivity [9]. Nonlinear acoustics has been widely used to probe material properties in many different fields, such as the nondestructive testing of single crystals and homogeneous small samples [19], geomaterials [11,20,21], biomaterials [10,12,22], and thin films [23]. Nonlinear behavior has been monitored using Rayleigh waves as well [24]. There appears to be a wide agreement in the literature that nonlinear methods are quite sensitive to small-scale inhomogeneities. Can nonlinear acoustics be used to monitor dislocation proliferation in metals and alloys?

2. Materials and Methods

The present article provides a quantitative assessment of linear versus nonlinear acoustic measurement of dislocation density in commercially pure copper and aluminum.

One nonlinear acoustic experimental method that is widely used as a non destructive evaluation tool is Second Harmonic Generation (SHG) [25]. In this method, a second harmonic wave is generated from a propagating monochromatic elastic wave, due to the anharmonicity of the elastic material and the presence of microstructural features such as dislocations. The second harmonic nonlinear response is quantified by

$$\beta = \frac{8}{xk^2} \frac{A_{2\omega}}{A_\omega^2}, \quad (2)$$

where k is the wave number, x is the elastic wave propagation distance, and A_ω and $A_{2\omega}$ are the absolute physical displacements of the fundamental and second harmonic waves [25].

A recent review [26] reports measurements of the amplitude of the second harmonic relative to the amplitude of the first harmonic, in samples of aluminum alloy and of steel before and after plastic elongation (0.2% in aluminum, 1.5% in low carbon steel). There is an unmistakable difference, at least in part attributable to the presumed difference in dislocation density. However, there does not appear to be an accepted model that quantitatively relates this unmistakable difference to a specific increase in dislocation density (see [26] and references therein).

As reported above, RUS relies on linear theory. It provides a complete set of elastic constants using one single measurement of the resonant spectrum in a given ultrasonic frequency range [27]. Extending the drive amplitude beyond the linear limit into the nonlinear regime one obtains Nonlinear Resonant Ultrasound Spectroscopy (NRUS), which is based on changes of one particular resonant

frequency [9–12,28]. The corresponding frequency shift $\Delta f = f_i - f_0$ is related phenomenologically with the average strain amplitude $\Delta\epsilon$ by the nonlinear parameter α , defined through

$$\frac{\Delta f}{f_0} = \alpha \Delta\epsilon = \alpha \gamma V_{rec} = \alpha' V_{rec}, \quad (3)$$

55 where f_0 is the resonant frequency in the linear regime. Here, we follow Payan [9]; instead of measuring
 56 the strain ϵ , we measure the pressure sensor voltage amplitude, V_{rec} , so we measure the nonlinear
 57 parameter α' , which will differ for samples with different dislocation densities. Also, we use the
 58 method of Johnson to account for the effect of temperature [29].

59 In this work, two groups of aluminum and copper samples have been used to perform RUS,
 60 NRUS, SHG, as well as X-ray diffraction (XRD), measurements, the latter as a control method. We
 61 show that the results using different acoustic methods are well correlated with those obtained by XRD
 62 peak broadening profile analysis. The relative sensitivity of RUS, NRUS and SHG are presented and
 63 we show that nonlinear parameters are more sensitive to the presence of dislocations than the linear
 64 ones.

65 99.999 at% pure aluminum and 99.95 at% pure copper samples were used to perform RUS, NRUS,
 66 SHG and XRD measurements. From the same as-received bar, four pieces were taken to prepare the
 67 experimental samples: all samples were cold-rolled at 82.8% and 88.3% in the aluminum and copper
 68 groups, respectively. Then, three samples of each group were annealed at about 70% of their melting
 69 point for 15, 30 and 60 min, labeled as Roll A15, Roll A30 and Roll A60 respectively. The sample without
 70 annealing was labeled only as Roll. It is well known that annealing leads to lower dislocation density,
 71 and stronger cold-rolling leads to higher dislocation density [17]. For each one of the four pieces
 72 per group, one portion was set aside for ultrasonic testing, and another two for XRD. For a correct
 73 application of RUS, the pieces must be modelable as perfect parallelepipeds to avoid resonance shifts
 74 [30]. The transverse wave speed v_T is measured with RUS. The Al samples we analyzed had average
 75 dimensions $(0.500 \pm 0.003) \times (1.704 \pm 0.003) \times (5.005 \pm 0.003) \text{ cm}^3$, and average density 2.667 ± 0.005
 76 gr/cm^3 . The Cu samples had average dimensions $(0.399 \pm 0.005) \times (1.701 \pm 0.001) \times (5.001 \pm 0.003)$
 77 cm^3 , and average density $8.891 \pm 0.010 \text{ gr/cm}^3$. Of course, precise measurements were made for
 78 each single sample in order to correctly apply the characterization methods. The XRD samples had
 79 dimensions $(1.704 \pm 0.003) \times (0.500 \pm 0.003)^2 \text{ cm}^3$ and $(1.701 \pm 0.001) \times (0.399 \pm 0.005)^2 \text{ cm}^3$ for the
 80 Al and Cu groups, respectively.

81 Both the linear and the nonlinear resonant ultrasound spectroscopy used the same setup [17,31].
 82 The positioning of the sample and its assembly conditions are the same as those described in [17].
 83 RUS is used to measure the shear wave velocity, because the shear modulus C_{44} can be determined
 84 with much higher accuracy. The drive amplitude is 1 V in the linear regime. The frequency sweep is
 85 performed between 26 kHz and 175 kHz, with 26 identified modes on average for Al. For Cu samples,
 86 the range of frequencies is 19 kHz to 127 kHz, with 21 identified modes on average. Ten independent
 87 measurements per sample were made to obtain associated statistical errors.

88 Imposing transverse isotropy, we have computed the anisotropy parameter $\epsilon = 1 - 2C_{44}/(C_{11} -$
 89 $C_{12})$ for both groups [32]; within experimental errors its is zero or very small for all samples.
 90 Additionally, we have computed the transverse wave speed imposing both isotropy and transverse
 91 isotropy in the RUS analysis and the differences obtained are $\lesssim 0.3\%$. XRD patterns show some degree
 92 of texture, which we have quantified using the March-Dollase model. The March-Dollase parameters
 93 for most reflections are close to 1. However, Cu peaks (220) and Al peaks (200) have parameters smaller
 94 than 1 but with small weight factors. We finally conclude that Al and Cu samples have a low degree of
 95 texture [33].

96 For NRUS application, the set up is exactly the same as for RUS. For both the Al and Cu groups,
 97 the resonance frequency that was chosen is close to 49 kHz and 39 kHz, respectively. The exact value
 98 depends on the specific dimensions of each sample. The reason for this choice was that the selected
 99 modes were the most energetic in the frequency range studied. In the non-linear regime, we verified

100 that the resonance is asymmetric and that its amplitude ceases to be a linear function of the excitation
101 voltage.

102 The third acoustic method used in this work is SHG. In this case the experimental setup for
103 non-linear ultrasonic measurements is simpler than for RUS and NRUS. A continuous sine wave of
104 frequency $f = 3$ MHz is transmitted into the material. Thus, a longitudinal wave is propagated across
105 the length $d \approx 1.7$ cm of each sample of both groups and the resulting response is analyzed for its
106 nonlinear features. Two equal transducers are placed on each side of the specimen (Panametrics - V110,
107 resonant at 5 MHz, with element diameter 8.8 mm). Through Fourier analysis of the received signal,
108 we measure the fundamental (A'_{ω}) and the second harmonic ($A'_{2\omega}$) amplitudes, in volts.

In general, the non-linear parameter is presented in units of 1/Volts [25]. This is because precise
transducer calibrations are difficult at such low driving amplitudes, which occur even in the non-linear
regime. Thus, following Matlack [25], instead of calculating β in dimensionless form we measure

$$\beta' = A'_{2\omega} / (A'_{\omega})^2, \quad (4)$$

109 which is based on the amplitudes measured in voltage units.

XRD measurements were carried out with the same procedure and equipment reported by Salinas
et al. [18] Microstructural parameters such as lattice parameter a and microstrain $\langle \epsilon^2 \rangle^{1/2}$, were obtained
from Rietveld refinements of the X-ray patterns with the Materials Analysis Using Diffraction (MAUD)
software and LaB_6 ($a = 4.1565915(1)$ Å) as external standard for the determination of instrumental
broadening. Using the information provided by MAUD, it is possible to obtain a measurement of
dislocation density Λ_{XRD} for each Al and Cu sample through

$$\Lambda_{XRD} = \frac{24\pi E \langle \epsilon^2 \rangle}{GF a^2}, \quad (5)$$

110 where $F \approx 5$ for FCC materials, E is Young's modulus and G is the shear modulus. The E and G values
111 used for Al were 74.4 ± 1.9 GPa and 28.1 ± 0.8 GPa, respectively. These values were calculated as an
112 average of those reported in [27,34,35]. For Cu, E and G used were 124.5 ± 0.7 GPa and 45.4 ± 1.2 GPa
113 respectively, obtained from [36]. We measured two pieces for the same sample of both groups, in order
114 to have an associated statistical error, beyond that provided by the refinement.

115 3. Results and discussion

116 Figure 1 shows an example of XRD pattern for an aluminum and copper sample. As in recent
117 works [18], there is not one crystallite size, but rather a distribution of sizes that contribute to each
118 diffraction peak, each one having an associated microstrain. Using the information about the volume
119 fraction of each phase provided by MAUD, the results for Λ were calculated as a weighted average of
120 results for different crystallite sizes.

121 The results of the acoustics measurements are given in Table 1, where the behavior of the linear
122 and nonlinear parameters is compared and contrasted. The linear parameter v_T shows variations
123 between purely rolled and annealed pieces between 1.7% and 2.6% for Al, and 2.9% and 4.4% for
124 Cu. The non-linear parameters are decreasing functions of the shear velocity v_T . This means they are
125 increasing functions of dislocation density. The parameter a' shows remarkable changes: 39% to 125%
126 for Al, and 320% to 510% for Cu. Finally, β' has variations from 14% to 20% for Al, and 19% to 62%
127 for Cu.

128 Dislocation density measurements are reported in Table 2. A RUS-determined dislocation density
129 Λ_{RUS} is obtained using Eqn. (1), together with a typical dislocation segment length $L \approx 150$ nm for Al
130 and $L \approx 230$ nm for Cu. The results for the shear wave velocity v_T reported above provide a variation
131 between samples of $\Delta\Lambda_{RUS} \approx (4 - 7) \times 10^7$ mm⁻² for the Al group and $\Delta\Lambda_{RUS} \approx (3 - 5) \times 10^7$
132 mm⁻² for the Cu group. In both cases the associated errors are less than 20%. The XRD-determined
133 dislocation density Λ_{XRD} , as expected, is lower for annealed samples than for purely rolled ones.

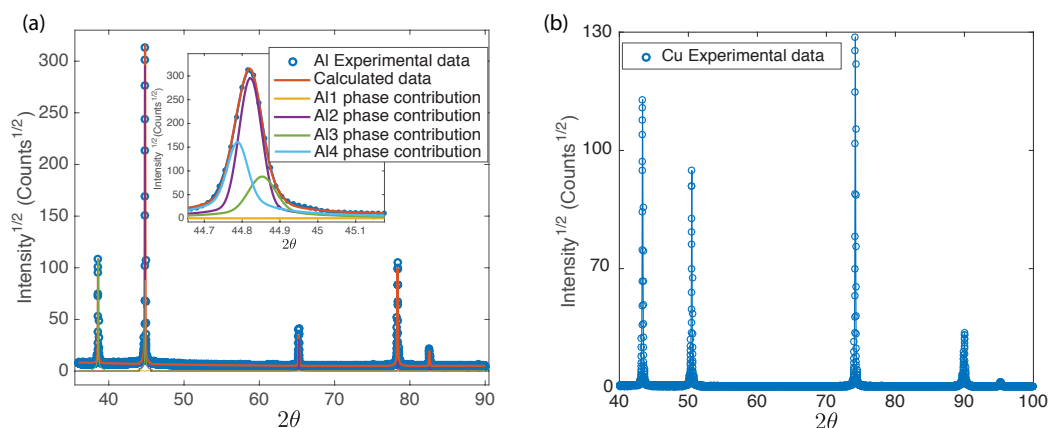


Figure 1. Example of (a) Aluminum and (b) Copper XRD pattern. (a) Five peaks are observed for Al, corresponding to different lattice planes: (111) ($2\theta = 38.55^\circ$), (200) ($2\theta = 44.81^\circ$), (220) ($2\theta = 65.21^\circ$), (311) ($2\theta = 78.35^\circ$) and (400) ($2\theta = 99.22^\circ$). Inset: A distribution of crystallite sizes (Al_{*i*}, $i = 1, 2, 3, 4$) contribute to the (200) diffraction peak (shown) as well as to the others (not shown). (b) For Cu samples, five peaks are observed in the angular range measured, corresponding to the following lattice planes: (111) ($2\theta = 43.37^\circ$), (200) ($2\theta = 50.51^\circ$), (220) ($2\theta = 74.2^\circ$), (311) ($2\theta = 90.01^\circ$) and (222) ($2\theta = 95.23^\circ$).

Table 1. Acoustic parameters, both linear and nonlinear, obtained for each group of samples compared and contrasted. Nonlinear parameters α' and β' exhibit a considerably higher change from sample to sample than the linear parameter v_T . Errors are obtained by standard deviation of ten measurements with each method. See text for symbol definition.

Aluminum			
Treatment	v_T (m/s)	$\frac{\alpha'}{10^{-4}}$ (V ⁻¹)	β' (V ⁻¹)
Roll A60	3116 ± 4	-39 ± 8	0.42 ± 0.02
Roll A30	3130 ± 7	-44 ± 7	0.39 ± 0.02
Roll A15	3146 ± 4	-63 ± 5	0.39 ± 0.02
Roll	3065 ± 4	-28 ± 5	0.49 ± 0.01
Copper			
Treatment	v_T (m/s)	$\frac{\alpha'}{10^{-4}}$ (V ⁻¹)	β' (V ⁻¹)
Roll A60	2294 ± 6	-168 ± 21	0.90 ± 0.10
Roll A30	2304 ± 4	-244 ± 31	0.35 ± 0.01
Roll A15	2326 ± 3	-176 ± 18	0.42 ± 0.01
Roll	2229 ± 4	-40 ± 10	1.11 ± 0.03

134 However, the associated errors are so large that it is not possible to clearly differentiate between
 135 pieces within each group. In any case, the values obtained are of the same order of magnitude of
 136 the acoustically obtained values so they do provide a check on the latter method. In Figure 2 we
 137 present the quantitative relation between the variations of the nonlinear parameters with respect to
 138 the changes in dislocation density. In a first approximation, we obtain that $\Delta\alpha'$ and $\Delta\beta'$ are linearly
 139 dependent of $\Delta\Lambda_{RUS}$. This method then provides a way to obtain dislocation density variations as
 140 function of the changes of the acoustic nonlinear parameters, with a high sensitivity compared to linear
 141 measurements. Thus, for a given material and once properly calibrated, one can indeed use the high
 142 sensitivity of the nonlinear parameters in order to quantitatively study dislocation proliferation in
 143 metals and alloys.

The nonlinear parameter β is defined through $\beta \equiv -[3 + (C_{111}/C_{11})]$ [25], with C_{11} and C_{111} the second- and third-order longitudinal elastic constants given by $\sigma = C_{11}\epsilon + (C_{111} + C_{11})\epsilon^2 + \dots$, where σ is stress and ϵ is strain. We already know [14] that n dislocation segments of length L per unit

Table 2. Comparison of XRD and RUS measurements of relative dislocation density for the Al and Cu samples. Errors for XRD measurements are calculated with the contribution of the Rietveld refinement results and the statistical error from the repetition of the experiment in two pieces of the same sample. These errors are large and preclude a sample-to-sample comparison. By contrast, the errors associated with the acoustic measurements are sufficiently small that a quantitative comparison can be confidently provided.

Aluminum		
Compared samples	$\frac{\Delta\Delta_{XRD}}{10^7}$ (mm ⁻²)	$\frac{\Delta\Delta_{RUS}}{10^7}$ (mm ⁻²)
Roll & Roll A60	1.24 ± 1.47	4.47 ± 0.70
Roll & Roll A30	0.87 ± 1.35	5.68 ± 0.96
Roll & Roll A15	0.42 ± 7.12	7.07 ± 0.69
Copper		
Compared samples	$\frac{\Delta\Delta_{XRD}}{10^7}$ (mm ⁻²)	$\frac{\Delta\Delta_{RUS}}{10^7}$ (mm ⁻²)
Roll & Roll A60	2.34 ± 21.74	3.31 ± 0.51
Roll & Roll A30	4.73 ± 19.35	3.81 ± 0.41
Roll & Roll A15	5.04 ± 19.0	4.90 ± 0.35

volume induce a change ΔC_{11} given by $\Delta C_{11}/C_{11} = -32\Delta(nL^3)/(45\pi^2)$. The influence of dislocations on β has been studied by several authors [37–41]. Since this influence is a small effect, one has that the change induced is proportional to dislocation density: $\Delta C_{111}/C_{111} = B\Delta(nL^3)$, with a dimensionless constant B that depends on the geometry and modeling employed. A simple calculation shows

$$\Delta\beta = - \left(\frac{\Delta C_{111}}{C_{111}} - \frac{\Delta C_{11}}{C_{11}} \right) \frac{C_{111}}{C_{11}}. \quad (6)$$

144 Since, for aluminum and copper $C_{111} \sim -10C_{11}$ [42], this formula provides, a rationale for
 145 understanding the factor of ten higher sensitivity of β to dislocation density, compared to the second
 146 order coefficient, as well as its increase, as long as $\Delta C_{111}/C_{111} > \Delta C_{11}/C_{11}$.

147 The parameter α depends on the coupling between the different normal modes of an elastic
 148 sample due to nonlinearities. Chakrapani and Barnard [43] have determined, both theoretically and
 149 experimentally, the value of α for a purely longitudinal mode of a thin beam, and have inferred that
 150 $\beta = -K\alpha$ with $K > 0$. Our measurements of α' and β' are consistent with this result (we remind that
 151 from Eqns. (3) and (4), we have $\alpha' \propto \alpha$ and $\beta' \propto \beta$). In particular, when the dislocation density increases
 152 the material is more nonlinear with respect to β , as it increases, but less nonlinear for α as it decreases
 153 in its absolute value. However, further investigation and modeling is needed to ascertain a precise
 154 formula for the influence of dislocations on the parameter α .

155 4. Conclusions

156 We have measured the change in the nonlinear parameters β' and α' as a function of the change in
 157 dislocation density in copper and aluminum, the change in dislocation density nL^3 being determined
 158 by linear acoustics. We have determined that a change of nL^3 by a factor of ten leads to a 20-60%
 159 change in β' , and to a factor of two to six change in α' . We also explain the difference in about a factor
 160 10 between the sensitivity of the linear and nonlinear measurements. These results pave the way for
 161 the use of nonlinear acoustics as a sensitive, quantitative, probe of dislocation density in metals and
 162 alloys.

163 **Author Contributions:** Conceptualization, C.E., C.A., R.E., F.L., V.S. and N.M.; Sample preparation, R.E.; RUS
 164 measurements and analysis, C.E., D.F. and N.M.; NRUS and SHG measurements and analysis, C.E., V.S. and N.M.;
 165 XRD measurements and analysis, C.E., V.S. and C.A.; writing, review and editing, C.E., C.A., R.E., F.L., V.S. and
 166 N.M.; funding acquisition, F.L., V.S., C.A., R.E. and N.M.

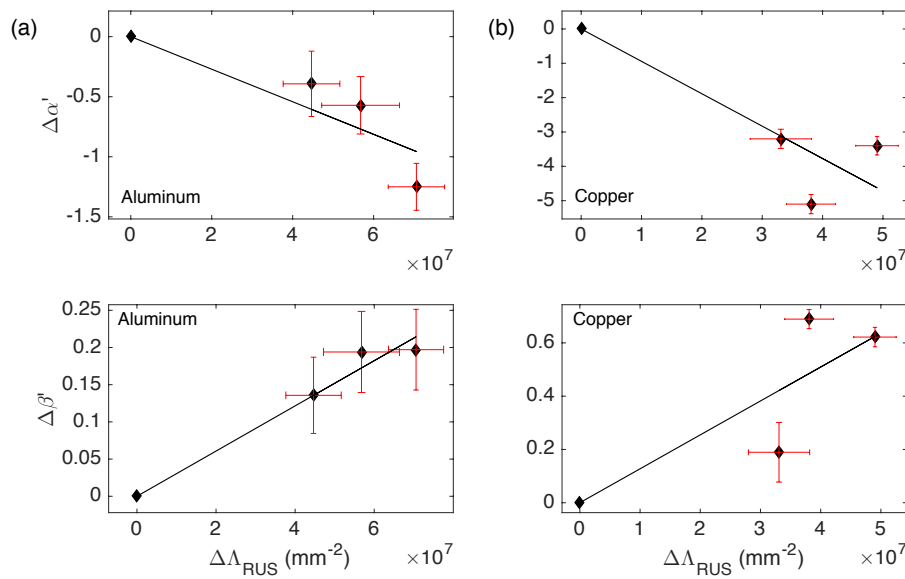


Figure 2. Normalized variations of nonlinear acoustic parameters α' and β' of each sample respect to the purely rolled one as functions of the variations of dislocation density, obtained with the linear measurements. For both groups Al and Cu, $\Delta\Lambda_{RUS}$ are similar, which are obtained from changes in the transverse elastic wave speed v_T , which are of the order of a few percent. (a) For the Al group, α' shows changes of 39% to 125% and β' of 14% to 20% (b) For the Cu group, α' shows changes of 320% to 510%, and β' of 19% to 62%.

167 **Funding:** This work was funded by Fondecyt Grant 1160823, Fondecyt Postdoctoral Grant 3160164 and
 168 FONDEQUIP EQM 140095.

169 **Conflicts of Interest:** The authors declare no conflict of interest.

170 Abbreviations

171 The following abbreviations are used in this manuscript:

172	RUS	Resonant ultrasound spectroscopy
	TEM	Transmission electron microscopy
173	XRD	X-ray diffraction
	SHG	Second harmonic generation
	NRUS	Nonlinear resonant ultrasound spectroscopy

174 References

- 175 1. Oh, S.H.; Legros, M.; Kiener, D.; Dehm G. In situ observation of dislocation nucleation and escape in a
 176 submicrometre aluminium single crystal. *Nat. Mater* **2009**, *8*(2), 95-100. doi:10.1038/nmat2370
- 177 2. Landau, P.; Schneck, R.Z.; Makov, G.; Venkert, A. In-situ TEM study of dislocation patterning
 178 during deformation in single crystal aluminum. *J. Phys. Conf. Ser.* **2010**, *241*(1), 012060.
 179 doi:10.1088/1742-6596/241/1/012060
- 180 3. Zhang, L.; Sekido, N.; Ohmura, T. Real time correlation between flow stress and dislocation density in steel
 181 during deformation. *Mater. Sci. Eng.* **2014**, *A 611*, 188-193. doi:10.1016/j.msea.2014.05.073
- 182 4. Du, J.; Mompou, F.; Zhang, W. -Z. In-situ TEM study of dislocation emission associated with austenite
 183 growth. *Scripta Materialia* **2018**, *145*, 62-66. doi:10.1016/j.scriptamat.2017.10.014
- 184 5. McSkimin, H.J. Pulse superposition method for measuring ultrasonic wave velocities in solids. *J. Acoust. Soc.*
 185 *Am.* **1961**, *33*, 12-16.
- 186 6. Chen, C.-H. *Ultrasonic and Advanced Methods for Nondestructive Testing and Material Characterization*; University
 187 of Massachusetts Dartmouth; USA, 2007. ISBN: 978-981-270-409-2.

- 188 7. Chanbi, D.; Ogam, E.; Amara, S.E.; Fellah, Z. Synthesis and Mechanical Characterization of Binary and
189 Ternary Intermetallic Alloys Based on Fe-Ti-Al by Resonant Ultrasound Vibrational Methods. *Materials* **2018**,
190 *11*, 746. doi:10.3390/ma11050746
- 191 8. Tiwari, K.A.; Raisutis, R. Identification and Characterization of Defects in Glass Fiber Reinforced Plastic by
192 Refining the Guided Lamb Waves. *Materials* **2018**, *11*, 1173. doi:10.3390/ma11071173
- 193 9. Payan, C.; Garnier, V.; Moysan, J.; Johnson, P.A. Applying nonlinear resonant ultrasound spectroscopy
194 to improving thermal damage assessment in concrete. *J. Acoust. Soc. Am.* **2007**, *121*(4), EL125-30.
195 doi:10.1121/1.2710745
- 196 10. Muller, M.; Sutin, A.; Guyer, R.A.; Talmat, M.; Laugier, P.; Johnson, P.A. Nonlinear resonant ultrasound
197 spectroscopy (nrus) applied to damage assessment in bone. *J. Acoust. Soc. Am.* **2005**, *118*, 3946-3952.
198 doi:10.1121/1.2126917
- 199 11. Payan, C.; Ulrich, T.J.; Le Bas, P.Y.; Saleh, T.; Guimaraes, M. Quantitative linear and nonlinear resonance
200 inspection techniques and analysis for material characterization: Application to concrete thermal damage. *J.*
201 *Acoust. Soc. Am.* **2014**, *136*, 537-546. doi:10.1121/1.4887451
- 202 12. Hauptert, S.; Guérard, S.; Mitton, D.; Peyrin, F.; Laugier, P. Quantification of nonlinear elasticity for the
203 evaluation of submillimeter crack length in cortical bone. *J. Mech. Behav. Biomed. Mater.* **2015**, *48*, 210-219.
204 doi:10.1016/j.jmbbm.2015.04.013
- 205 13. Maurel, A.; Pagneux, V.; Barra, F.; Lund, F. Ultrasound as a probe of plasticity? The interaction of elastic
206 waves with dislocations. *Int. J. Bifurcat. Chaos* **2009**, *19*(8), 2765-2781. doi:10.1142/S0218127409024475
- 207 14. Maurel, A.; Pagneux, V.; Barra, F.; Lund, F. Wave propagation through a random array of pinned dislocations:
208 Velocity change and attenuation in a generalized Granato and Lücke theory. *Phys. Rev. B: Condens. Mater.*
209 **2005**, *72*, 174111. doi:10.1103/PhysRevB.72.174111
- 210 15. Granato, A.; Lücke, K. Theory of Mechanical Damping Due to Dislocations. *Journal of Applied Physics* **1956**,
211 *27*, 583. doi:10.1063/1.1722436
- 212 16. Migliori, A.; *U. S. Patent*; Patent number: 5.062.296, 1991.
- 213 17. Mujica, N.; Cerda, M.T.; Espinoza, R.; Lisoni, J.; Lund, F. Ultrasound as a probe of dislocation density in
214 aluminum. *Acta Mater.* **2012**, *60*, 5828-5837. doi:10.1016/j.actamat.2012.07.023
- 215 18. Salinas, V.; Aguilar, C.; Espinoza-González, R.; Lund, F.; Mujica, N. In situ monitoring of dislocation
216 proliferation during plastic deformation using ultrasound. *Int. J. Plast.* **2017**, *97*, 178-193.
217 doi:10.1016/j.ijplas.2017.06.001
- 218 19. Migliori, A.; Maynard, J.D. Implementation of a modern resonant ultrasound spectroscopy system for
219 the measurement of the elastic moduli of small solid specimens. *Rev. Sci. Inst.* **2018**, *76*, 121301.
220 doi:10.1063/1.2140494
- 221 20. Ulrich, T.J.; McCall, K.R.; Guyer, R. A.; Determination of elastic moduli of rock samples using resonant
222 ultrasound spectroscopy. *J. Acoust. Soc. Am.* **2002**, *111*, 1667-1674. doi:10.1121/1.1463447
- 223 21. Johnson, P.A.; Guyer, R.A.; Ostrovsky, L.A. Nonlinear mesoscopic elastic class of materials. Proceedings of
224 the International Symposium on Nonlinear Acoustics, Göttingen, Germany, September 1-4, 1999.
- 225 22. Kinney, J.H.; Gladden, J.R.; Marshall, G.W.; Marshal, S.J.; So, J.H.; Maynard, J.D. Resonant ultrasound
226 spectroscopy measurements of the elastic constants of human dentin. *J. Biomech.* **2004**, *37*, 437-441.
227 doi:10.1016/j.jbiomech.2003.09.028
- 228 23. Nakamura, N.; Ogi, H.; Hirao, M. Resonance ultrasound spectroscopy with laser-Doppler interferometry for
229 studying elastic properties of thin films. *Ultrasonics* **2004**, *42*, 491-494. doi:10.1016/j.ultras.2004.01.048
- 230 24. Herrmann, J. Assessment of material damage in a nickel-base superalloy using nonlinear Rayleigh surface
231 waves. *J. Appl. Phys.* **2006**, *99*, 124913. doi:10.1063/1.2204807
- 232 25. Matlack, K.H.; Kim, J.Y.; Jacobs, L.J.; Qu, J. Review of Second Harmonic Generation Measurement Techniques
233 for Material State Determination in Metals. *J. Nondestruct. Eval.* **2015**, 34-273. doi:10.1007/s10921-014-0273-5
- 234 26. Hirao, M.; Ogi, H. *Electromagnetic Acoustic Transducers*. Springer Japan, Japan, 2017; pp. 209-216; ISBN
235 978-4-431-56036-4.
- 236 27. Ogi, H.; Sato, K.; Asada, T.; Hirao, M. Complete mode identification for resonance ultrasound spectroscopy.
237 *J. Acoust. Soc. Am.* **2002**, *112*(6), 2553-2557. doi:10.1121/1.1512700
- 238 28. Van Den Abeele, K.; Carmeliet, J.; Ten Cate, J.A.; Johnson, P.A. Nonlinear elastic wave spectroscopy (NEWS)
239 techniques to discern material damage. Part II: Single-mode nonlinear resonance acoustic spectroscopy. *Res.*
240 *Nondestruct. Eval.* **2000**, *12*(1), 31-42. doi:10.1080/09349840009409647

- 241 29. Hauptert, S.; Renaud, G.; Riviere, J.; Talmant, M.; Johnson, P. A.; Laugier, P. High-accuracy acoustic detection
242 of nonclassical component of material nonlinearity. *J. Acoust. Soc. Am.* **2011**, *130*(5), 2664-2661. doi:
243 10.1121/1.3641405
- 244 30. Spoor, P.S. Elastic Properties of novel materials using PVDF film and Resonant Acoustic Spectroscopy. Ph. D.
245 Thesis, The Pennsylvania State University, 1996.
- 246 31. Espinoza, C. Caracterización de densidad de dislocaciones mediante espectroscopía de resonancia ultrasónica
247 no lineal. M. Sc. Thesis, Universidad de Chile, 2013.
- 248 32. Spoor, P.S.; Maynard, J.D.; Kortan, A.R. Elastic Isotropy and Anisotropy in Quasicrystalline and Cubic
249 AlCuLi. *Phys. Rev. Lett.* **1995**, *75*, 3462. doi:10.1103/PhysRevLett.75.3462
- 250 33. Zolotoyabko, E. Fast quantitative analysis of strong uniaxial texture using a March-Dollase approach. *J. Appl.*
251 *Cryst.* **2013**, *46*, 1877-1879. doi:10.1107/S0021889813027738
- 252 34. Lincoln, R.C.; Koliwad, K.M.; Ghate, P.B. Morse-Potential Evaluation of Second- and Third-Order Elastic
253 Constants of Some Cubic Metals. *Phys. Rev., Second Series* **1967**, *157*(3), 463-466. doi:10.1103/PhysRev.157.463
- 254 35. Vallin, J.; Mongy, M.; Salama, K.; Beckman, O. Elastic Constants of Aluminum. *J. Appl. Phys.* **1964**, *35*,
255 1825-1826. doi:10.1063/1.1713749
- 256 36. Ledbetter, H.M.; Naimon, E. R. Elastic Properties of Metals and Alloys. II. Copper. *J. Phys. Chem. Ref. Data*
257 **1974**, *3*(4), 897-935. doi:10.1063/1.3253150
- 258 37. Cantrell, J.H. Nonlinear dislocation dynamics at ultrasonic frequencies. *J. Appl. Phys.* **2009**, *105*, 043520.
259 doi:10.1063/1.3081972
- 260 38. Suzuki, T.; Hikata, A.; Elbaum, C. Anharmonicity Due to Glide Motion of Dislocations. *J. Appl. Phys.* **1964**,
261 *35*, 2761. doi:10.1063/1.1713837
- 262 39. Cash, W.D.; Cai, W. Dislocation contribution to acoustic nonlinearity: The effect of orientation-dependent
263 line energy. *J. Appl. Phys.* **2011**, *109*, 014915. doi:10.1063/1.3530736
- 264 40. Zhang, J.; Xuan, F.; Xiang, Y. Dislocation characterization in cold rolled stainless steel using
265 nonlinear ultrasonic techniques: A comprehensive model. *Europhys. Lett.* **2013**, *103*, 68003.
266 doi:10.1209/0295-5075/103/68003
- 267 41. Zhang, J.; Xuan, F. A general model for dislocation contribution to acoustic nonlinearity. *Europhys. Lett.* **2014**,
268 *105*, 54005. doi:10.1209/0295-5075/105/54005
- 269 42. Lubarda, V.A. New estimates of the third-order elastic constants for isotropic aggregates of cubic crystals. *J.*
270 *Mech. Phys. Solids.* **1997**, *45*(4), 471490. doi:10.1016/S0022-5096(96)00113-5
- 271 43. Chakrapani, S.K.; Barnard, D.J. Determination of acoustic nonlinearity parameter (β) using nonlinear
272 resonance ultrasound spectroscopy: Theory and experiment. *J. Acoust. Soc. Am.* **2017**, *141*(2), 919. doi:
273 10.1121/1.4976057